mater.scichina.com link.springer.com

Published online 19 June 2020 | https://doi.org/10.1007/s40843-020-1364-4
Sci China Mater 2020, 63(10): 2028–2039

Flexible fabric gas sensors based on PANI/WO_3 p–n heterojunction for high performance NH_3 detection at room temperature

Meng He[1,2†], Lili Xie[2†], Guifang Luo[2], Zhanhong Li[2], James Wright[3] and Zhigang Zhu[1,2*]

ABSTRACT **A PANI/WO_3@cotton thread-based flexible sensor that is capable of detecting NH_3 at room temperature is developed here. A layer of WO_3 with PANI nanoparticles can be deposited by *in-situ* polymerization. The morphology and structure of the specimens were investigated by utilizing TEM, SEM, XRD and FTIR. The sensing performance of the PANI/WO_3@cotton sensors with different WO_3 molar ratios to NH_3 at room temperature was examined. The results show that the optimal sensor (10 mol% WO_3) has a response of 6.0 to 100 ppm NH_3, which is significantly higher than that of the sensors based on pristine PANI and other composites. The PANI/WO_3@cotton sensor also displays excellent selectivity, gas response, and flexibility even at room temperature. The unique fiber structure, p-n heterojunction, and the increased protonation of PANI in the composites contribute to the enhanced sensing property.**

Keywords: gas sensor, PANI/WO_3 cotton thread, p-n heterojunction, NH_3 detection

INTRODUCTION

Ammonia (NH_3) is a colorless gas with strong pungent odors, usually released from nitrogenous plants and animals, organic decomposition, industrial waste-water, and motor vehicles [1]. Inhalation of NH_3 in a short time can cause acute respiratory diseases such as laryngitis, trachea bronchitis, bronchopneumonia, and even pulmonary edema [2]. Long-term exposure to NH_3 even at low concentration can irritate human eyes and skin. In terms of occupational exposure limits for hazardous agents in the workplace, the maximum allowable concentration for NH_3 is 40 ppm [3], while the detection limit of human olfaction is 25 ppm. Thus, it is desired to develop NH_3 sensors with high gas response and low detection limit for environmental analysis, chemical industry, and medical applications [4–6].

In recent years, many different materials have been developed and employed for the detection of toxic gases, including metal oxide semiconductors [7–9], conductive polymers [10,11], carbon nanomaterials [12, 13], halides [14], molecular sieves [15], metal-organic frameworks [16] and hybrid materials [17]. Among them, conductive polymers have been extensively studied for their excellent properties, such as ease of synthesis and modification, and operation at room temperature [6]. Polyaniline (PANI) is one of the ideal candidates due to its high conductivity, reversible doping/de-doping, good environmental stability and admirable selectivity to ammonia [18–21]. Nano-sized PANI with high surface-to-volume ratio and unique electrical properties can enhance the gas adsorption/desorption and thus promote the response and recovery processes [18]. However, the gas sensors based on pure conductive polymers exhibit poor sensing performance, mainly because low temperature and high humidity affect the stability of polymer materials [22,23]. To address this issue, researchers have attempted to combine PANI with metal oxide semiconductors to improve NH_3 sensing performance at low operating temperature [24,25]. The hybrid material not only retains the high performance of the metal oxide semiconductor, but also can lower the operating temperature and increase the flexibility originating from the conductive polymer. Bandgar *et al.* [26] prepared camphor sulfonic acid-doped PANI/α-Fe_2O_3 composite films

[1] School of Medical Instrument and Food Engineering, University of Shanghai for Science and Technology, Shanghai 200093, China
[2] School of Environmental and Materials Engineering, Shanghai Polytechnic University, 2360 Jinhai Road, Shanghai 201209, China
[3] Department of Electronic Engineering, School of Engineering, Technological University Dublin, Tallaght, Dublin 24, Ireland
† These authors contributed equally to this work.
* Corresponding author (email: zhigang_zhu259@163.com)

using an *in-situ* polymerization process, which displayed high selectivity and rapid response to NH_3 at room temperature. Wang *et al.* [27] reported that the NH_3 gas sensor based on PANI@CeO_2 exhibited both high response and long-term stability. SnO_2/PANI nanosheets-based sensor displayed a high response to NH_3 with a low detection limit [28]. In view of the above studies, polymer/metal oxide composites can improve their ammonia detection performance. Moreover, conductive polymers are relatively easier to assemble with flexible materials to construct flexible gas sensors [29,30].

A typical n-type tungsten oxide (WO_3) has been widely used as gas-sensing materials due to the tunable resistance, easy synthesis, low cost and environment-friendly properties [31,32]. Szilagyi and co-authors [33] indicated hexagonal WO_3-based sensor could detect ppm levels of NH_3 at 300°C. Srivastava *et al.* [34] introduced a two-layer sensor structure with different noble metals, exhibiting the improved gas response and reduced response time for NH_3 detection. Herein, we combined the advantages of WO_3, PANI and cotton thread to construct a flexible gas sensor, displaying a strong response to NH_3. The PANI/WO_3@cotton threads were obtained by *in-situ* chemical deposition, and the p-n junction at the interface between WO_3 and PANI was formed. The assembled flexible PANI/WO_3@cotton thread-based gas sensor exhibits excellent sensing characteristics such as high gas response, fast response with appropriate recovery, excellent repeatability and selectivity at room temperature. The gas response of PANI/WO_3 thread is better than that of pristine PANI, mainly due to the formation of the p-n heterojunction between PANI and WO_3 and the improved protonation of PANI by WO_3.

EXPERIMENTAL SECTION

Synthesis of materials

All chemicals were of analytical reagent grade from Sinopharm Chemical Reagent Co. Ltd, and utilized as received. The preparation of WO_3 was according to our previous work [35], and the specific procedure was as follow. $Na_2WO_4{\cdot}2H_2O$ (1.0 g) and 0.2 g of $H_2C_2O_4{\cdot}2H_2O$ were dissolved in 20 mL deionized water and evenly mixed through sonication for 5 min. Then, 3 mol L^{-1} hydrochloric acid was added dropwise to the above solution and stirred for 3 h. The reaction mixture was transferred to a stainless steel autoclave and heated at 180°C for 15 h. Finally, the reaction mixture was centrifuged at 8000 rpm for 10 min and then washed with deionized water and followed by ethanol three times. A yellow-green powder was obtained after drying at 60°C in an oven.

Fabrication of PANI/WO_3@cotton thread sensor

The PANI/WO_3@cotton thread sensor was fabricated by means of chemical oxidation polymerization. Aniline (2 mmol) and different amounts of WO_3 were dispersed in 20 mL of sulfosalicylic acid (SSA, $C_7H_6O_6S{\cdot}2H_2O$, 0.1 mol L^{-1}) solution and ultrasonicated for 30 min to form homogeneous suspension. Subsequently, commercially available cotton threads pretreated with ethanol and deionized water were immersed in the above solution. Meanwhile, 2 mmol of ammonium persulfate (APS) was added to 20 mL of SSA solution (0.1 mol L^{-1}) and pretreated in an ice water bath for 30 min, to obtain a mixture of APS/SSA. Then, the APS/SSA mixture was added to the above suspension and polymerized in the ice bath for 2 h. A schematic illustration of the synthesis process is presented in Fig. 1. The precipitate was centrifuged at 8000 rpm for 5 min and then washed thrice. The PANI/WO_3 nanomaterials were dried at 60°C overnight. The PANI/WO_3@cotton thread was washed with deionized water and ethanol thrice to ensure the removal of reactants. For convenience, we defined the PANI/WO_3 composites with various molar ratios as S1, S2, S3 and S4, which can be found in Fig. 1.

Characterization

The phase and crystallinity were characterized by X-ray diffraction (XRD) using a monochromatized Cu target (D8-Advance, Bruker, Germany). The morphology of the samples was examined by field emission scanning electron microscopy (FESEM, S-4800, Hitachi Co. Ltd, Japan), accelerated at 10 kV. The elemental distribution of the crystals was investigated by an energy dispersive X-ray spectrometer (EDX), affiliated to the SEM. A transmission electron microscope (TEM, JEM-2100F, JEOL Co. Ltd., Japan) was employed to observe the sample microstructure, accelerated at 200 kV. Fourier transform infrared (FTIR) spectroscopy was selected to investigate the chemical structure of the composites with a wavenumber range of 500–4000 cm^{-1} (L1600400, PerkinElmer Co., Ltd. England).

Gas-sensing performance

The PANI/WO_3@cotton thread was tested using an approximate length of 2 cm on each occasion. Before the test, the cotton thread should be dried overnight at a constant temperature and humidity to reduce the moisture content on the sensor surface. The gas response

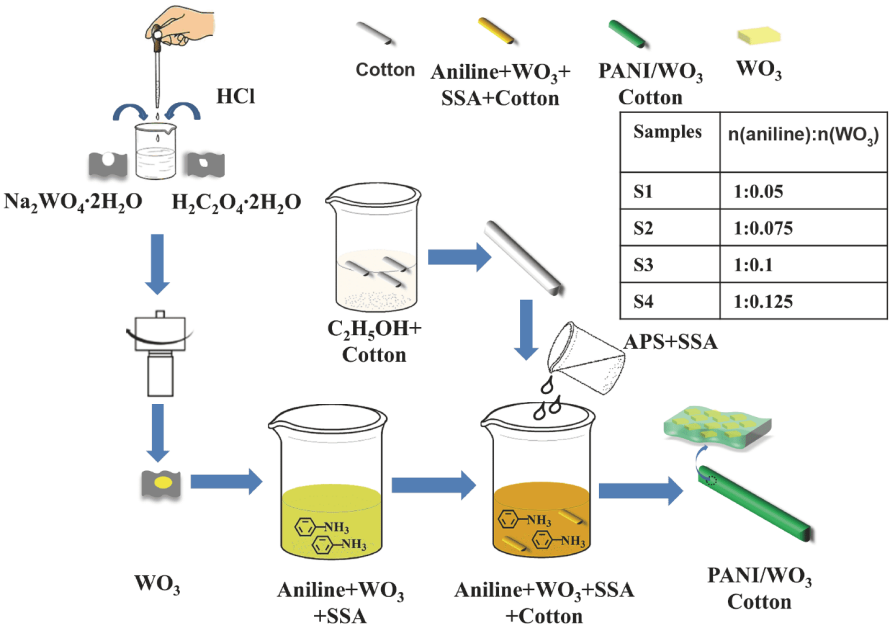

Samples	n(aniline):n(WO_3)
S1	1:0.05
S2	1:0.075
S3	1:0.1
S4	1:0.125

Figure 1 Schematic illustration of the preparation procedure for PANI/WO_3@cotton thread.

of the sensor was tested using a CGS-8 testing system (Beijing Elite Technology Co., Ltd. China), and defined as the ratio of the resistance of the sensor in the target gas (R_g) and the resistance (R_a) determined in the air ($S=R_g/R_a$), with the operating temperature at 28°C. The response time was defined as the time taken for the change of resistance to 90% of the equilibrium value once the testing gas was introduced, while the recovery time was the time for the resistance to return its 10% original value once the air was injected [36].

RESULTS AND DISCUSSION

Structure and morphology analysis

The XRD patterns of the pristine PANI, WO_3, and PANI/WO_3 composites are displayed in Fig. 2. The pristine PANI (curve a) demonstrates broad and weak diffraction peaks around 2θ=12° and 22°, and a sharper crest at 2θ =26°, which implies the amorphous structure of the PANI [3]. The pristine WO_3 (curve c) illustrates well-defined diffraction peaks at 23.12°, 23.59°, 24.38°, 26.59°, 28.94°, 33.27°, 34.16°, 35.67°, 41.44°, 49.95°, and 55.96°, corresponding to the (002), (020), (200), (120), (112), (022), (202), (122), (−222), (140) and (420) planes of monoclinic WO_3 (JCPDS No. 83-0951), respectively. No other phases were found, indicating the high purity of the synthesized WO_3. The XRD pattern (curve b) of the PANI/WO_3 composite shows the distinct peaks of WO_3, but the peaks

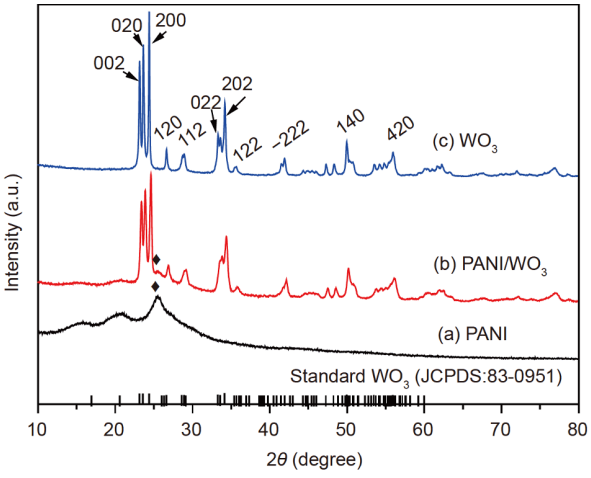

Figure 2 XRD patterns of the samples: (a) PANI, (b) PANI/WO_3 composites, and (c) WO_3.

are weaker than those of the pristine WO_3, due to the formation of PANI/WO_3 composite [3]. Moreover, the absorption line fluctuates at 2θ=15~30°, which is similar to that of the pristine PANI.

The morphologies of WO_3, PANI/WO_3 composites, PANI/WO_3@cotton thread, and PANI were observed by FESEM, as presented in Fig. 3. In Fig. 3a, the WO_3 are nano-blocks of 650 nm×650 nm×50 nm with a flat and smooth surface. Fig. 3b presents the PANI/WO_3 composites, which exhibit rough surface nano-blocks sur-

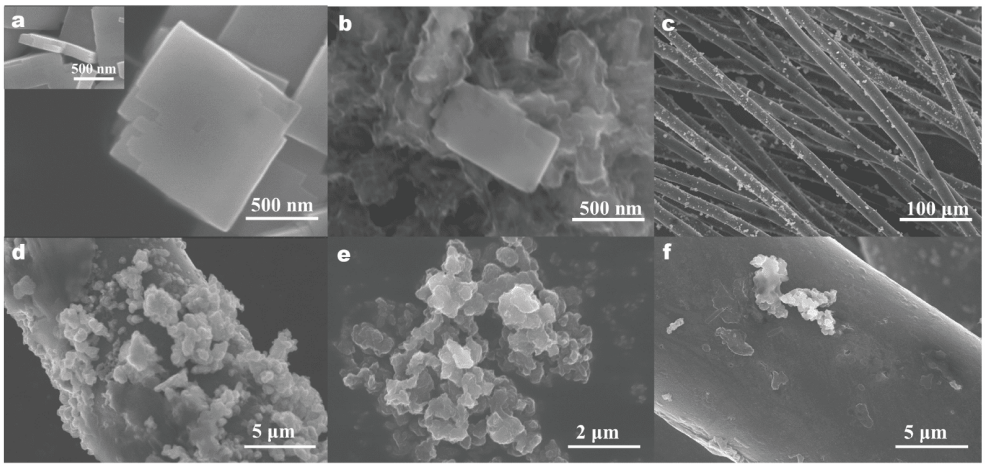

Figure 3 FESEM images of the samples: (a) WO_3, (b) PANI/WO_3 composites (S3), (c and d) PANI/WO_3@cotton thread (S3), (e) pristine PANI, and (f) PANI decorated cotton thread.

rounded by numerous PANI nanoparticles. The FESEM images of cotton thread treated with PANI/WO_3 are shown in Fig. 3c, d, and the PANI/WO_3@cotton thread displays a rough surface, decorated by nanoparticles with various sizes. To study the effect of the PANI/WO_3 molar ratios on the sensing performance, three other PANI/WO_3 cotton threads were synthesized. As shown in Fig. 4a–c, with the increase of the amount of WO_3, more aniline molecules are needed to wrap the cotton thread and WO_3. After the polymerization reaction, the size of individual PANI nanoparticles on the surface of the cotton thread decreases. The morphologies of PANI are nanoflakes with irregular size and shape, which prominently agglomerate together (Fig. 3e). Fig. 3f shows the pristine PANI treated cotton thread has a smooth surface, implying that without WO_3, only a small amount of PANI nanoparticles adhere to the cotton thread, resulting in a non-homogeneous PANI coating.

The elemental composition of the PANI@cotton thread and PANI/WO_3@cotton thread can be quantitatively analyzed by using EDX, as shown in Fig. 5. Compared with the pristine PANI@cotton thread, the PANI/WO_3@cotton thread possesses the main elements of C, N, O, S and W. Since the PANI was modified with SSA during the preparation process, the S element appears in both specimens. The atomic percentages of C, N, O, and S elements in the PANI@cotton thread are 41.94%, 36.64%, 21.36%, and 0.06%, respectively. For the PANI/WO_3@cotton thread, the ratios of C, N, O, S and W elements are 40.89%, 35.65%, 22.94%, 0.17%, and 0.35% respectively. It is clear that the atomic proportions of the C and O elements in both types of cotton threads are quite similar, but the atomic proportion of the S element for the PANI@cotton thread is significantly higher than that in the PANI/WO_3@cotton thread. This indicates that the combination of PANI and WO_3 improves the protonation degree of PANI, which will be further discussed later.

TEM was used to acquire more information about the morphology and structure of WO_3 and PANI/WO_3. TEM images confirm the nano-blocks feature of the WO_3, as shown in Fig. 6a, entirely consistent with the FESEM results. Fig. 6b, c reveal that the translucent PANI decorate on the surface of the WO_3 nanosheets. This is consistent with the results obtained by FESEM, where the polymerized PANI is well combined with the WO_3 nanosheets. Fig. 6d displays an high resolution TEM

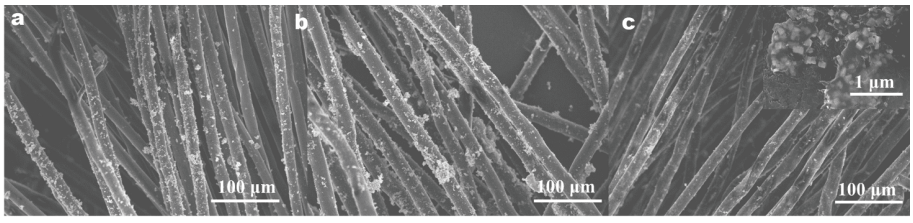

Figure 4 FESEM images of samples with different molar ratios: (a) S1 (5%), (b) S2 (7.5%), and (c) S4 (12.5%).

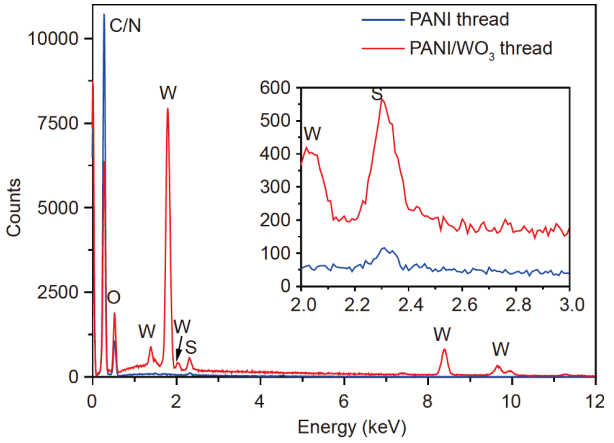

Figure 5 EDX spectra of PANI@cotton thread and PANI/WO_3@cotton thread.

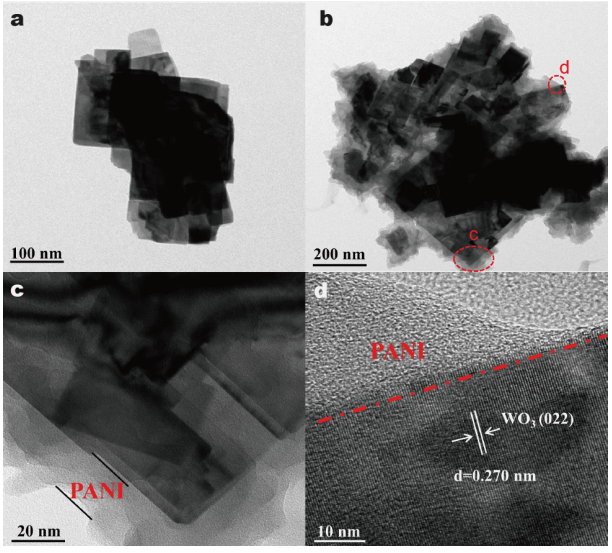

Figure 6 TEM images of (a) WO_3, (b and c) PANI/WO_3 composites, and (d) HRTEM of PANI/WO_3 composites.

(HRTEM) image of the PANI/WO_3 composite with the fringe distances of 0.270 nm corresponding well with the lattice distance of the (022) plane of monoclinic WO_3 [37]. Besides, a distinct boundary is between the WO_3 nanosheet and the PANI (Fig. 6d), suggesting that a p-n heterojunction might be formed between the WO_3 and PANI.

The chemical structures of the pristine PANI, PANI/WO_3 composites, and WO_3 were analyzed by using FTIR, as presented in Fig. 7 within 500–4000 cm^{-1}. The peaks at 1560, 1478, 1300, 1242, 1123 and 800 cm^{-1} are mainly attributed to the distinctive absorption peaks of the pristine PANI (curve a) [38]. Furthermore, the peak lo-

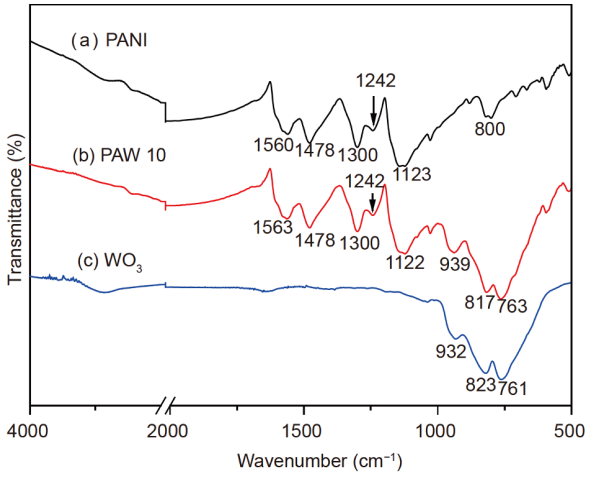

Figure 7 FTIR spectra of (a) PANI, (b) PANI/WO_3, and (c) WO_3.

cated at 1560 cm^{-1} is related to the N=Q=N stretching vibration in the quinoid structure, and the peak at 1478 cm^{-1} corresponds to the N=B=N vibration of the benzenoid structure. The vibration peaks of C–N, and C=C are at 1300 and 1242 cm^{-1}, respectively [39]. The peaks at 1123 and 800 cm^{-1} can be assigned to C–H stretching vibration within and outside of the plane [40]. The characteristic peaks of WO_3 (curve c) are located at 932, 823 and 761 cm^{-1} and the distinctive bands at 823 and 761 cm^{-1} are recognized as the W–O–W stretching vibrations of WO_3 [41]. The characteristic spectrum of the PANI/WO_3 composite is presented in curve b. The PANI/WO_3 composite shows five vibration peaks of PANI at 1563, 1478, 1300, 1242, and 1122 cm^{-1} as well as three main peaks of WO_3 at 939, 817 and 763 cm^{-1}, indicating a successful combination of the PANI and WO_3.

XPS measurements were carried out to study the chemical states and elemental composition of the PANI/WO_3 and PANI/WO_3@cotton thread. For the full spectra in Fig. 8a, the characteristic peaks of W, S and O elements coexist in the PANI/WO_3 and PANI/WO_3@cotton thread. The detailed chemical states of W, S and O elements are shown in the corresponding fine spectra. In Fig. 8b, W 4f spectrum of the PANI/WO_3 clearly shows two characteristic peaks at 35.7 and 37.8 eV with a spin-orbit interval of 2.1 eV, which are assigned to W $4f_{7/2}$ and W $4f_{5/2}$ with the +6 oxidation state, respectively [42]. These two characteristic peaks shift to 35.5 and 37.6 eV for the PANI/WO_3@cotton thread. Compared with PANI/WO_3, the W 4f binding energy shifts of the PANI/WO_3@cotton thread are ascribed to the charge transfer between PANI/WO_3 and cotton thread due to the formed close contacts at the interface [43]. In Fig. 8c, the high-

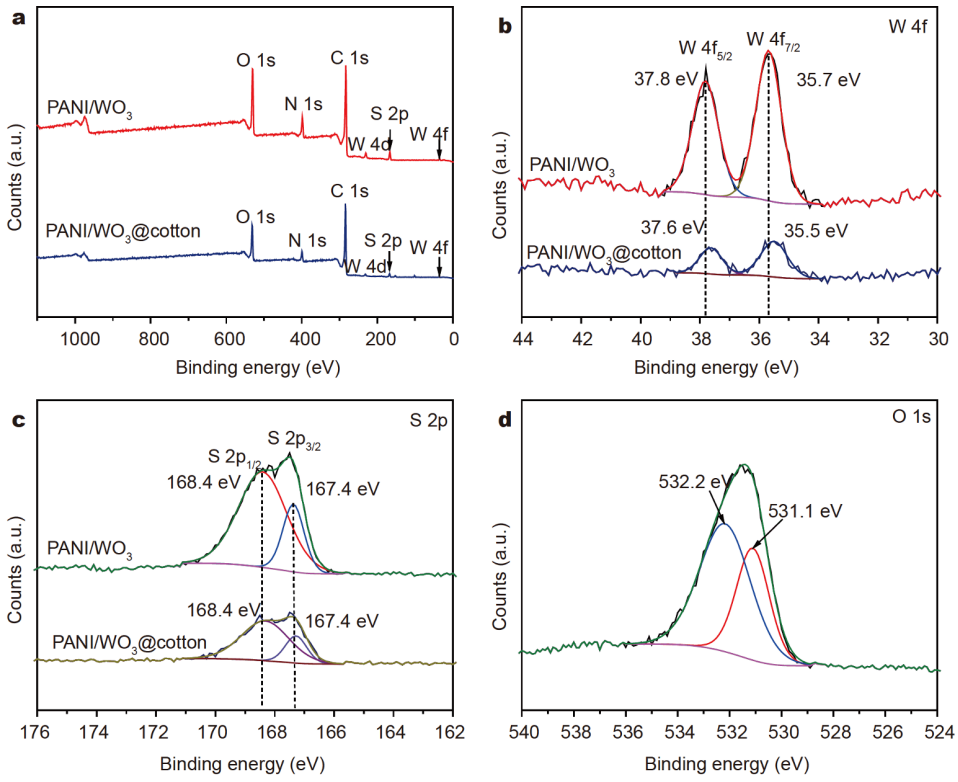

Figure 8 XPS spectra of PANI/WO_3 powder and PANI/WO_3@ cotton thread: (a) full spectra, (b) W 4f, (c) S 2p and (d) O 1s.

resolution S 2p spectra can be well deconvoluted into two peaks at 167.4 and 168.4 eV, corresponding to S $2p_{3/2}$ and S $2p_{1/2}$ states, respectively. The formation of S element is attributed to the added SSA and ammonium persulfate during the synthesis process. For the O element in Fig. 8d, the binding peaks at 531.1 and 532.2 eV are ascribed to W–O and the adsorbed oxygen (O^{2-}, O^{-}) on the surface of WO_3, respectively [44].

The sensing properties

One merit of this work is the selection of cotton thread as the flexible substrate. As high working temperature during conventional sensing test will damage the thread, therefore, all the sensing test was conducted at room temperature. The gas response of the pristine PANI thread and PANI/WO_3 cotton thread to 100 ppm NH_3 was investigated at room temperature. As presented in Fig. 9, the gas responses ($S=R_g/R_a$) of the PANI@cotton thread is 2.5. The gas response of the PANI/WO_3@cotton sensors with different PANI/WO_3 molar percentages show an "increased-maximum-reduced" trend. In the case of pristine WO_3, the sensor responds weakly to 100 ppm NH_3 at room temperature. When the WO_3

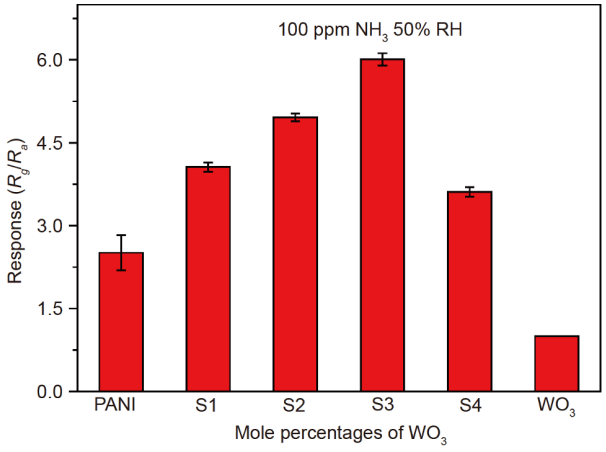

Figure 9 The effect of the WO_3 mole percentage (S1: 5%, S2: 7.5%, S3: 10%, S4: 12.5%) on the sensing response of sensors to 100 ppm NH_3.

molar percentage is 10%, the PANI/WO_3@cotton sensor achieves the highest response value of 6.0, demonstrating that the sample with a mole percentage of 10% WO_3 exhibits better performance to NH_3 than that of 12.5%. The reasons are as follow: first, as the WO_3 molar percentage increases to 12.5%, some WO_3 nanoparticles

cannot be fully coated by PANI and directly decorate on the cotton surface (Fig. 4c), affecting the reaction between protonated PANI and NH_3. Second, the excessive electrons from WO_3 make the depletion region thicker at the hetero-interface, thereby reducing the sensing performance. Therefore, a large amount of WO_3 addition results in a deterioration of the response of the PANI/WO_3@cotton sensor to NH_3.

Selectivity refers to the ability of the sensor to accurately identify the target gas, which is a highly important characteristic of the gas sensor [45]. Fig. 10 illustrates the selectivity of a PANI/WO_3@cotton sensor for various testing gases, such as NH_3, CO, ethanol, H_2S, acetone, toluene, xylene, and NO_2, at the concentration of 100 ppm. The results demonstrate that the PANI/WO_3@cotton sensor displays the highest gas response (6.0) to NH_3, while the response values to other interference gases are in the range of 1.01–1.30, confirming the excellent selectivity of the PANI/WO_3@cotton thread-based sensor for NH_3 detection.

Response/recovery time is one of the important factors for characterizing sensor performance, as rapid response and recovery processes facilitate real-time detection. Moreover, the reversible ability during the adsorption/desorption processes is crucial for a flexible fabric sensor in the real application. Fig. 11a displays the transient response-recovery curve of the PANI/WO_3 cotton thread sensor to 100 ppm NH_3 at room temperature. The results

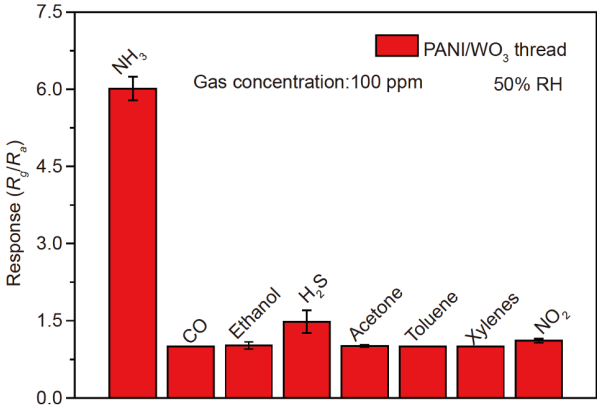

Figure 10 The selectivity of the PANI/WO_3@cotton thread sensor to various gases of 100 ppm at room temperature.

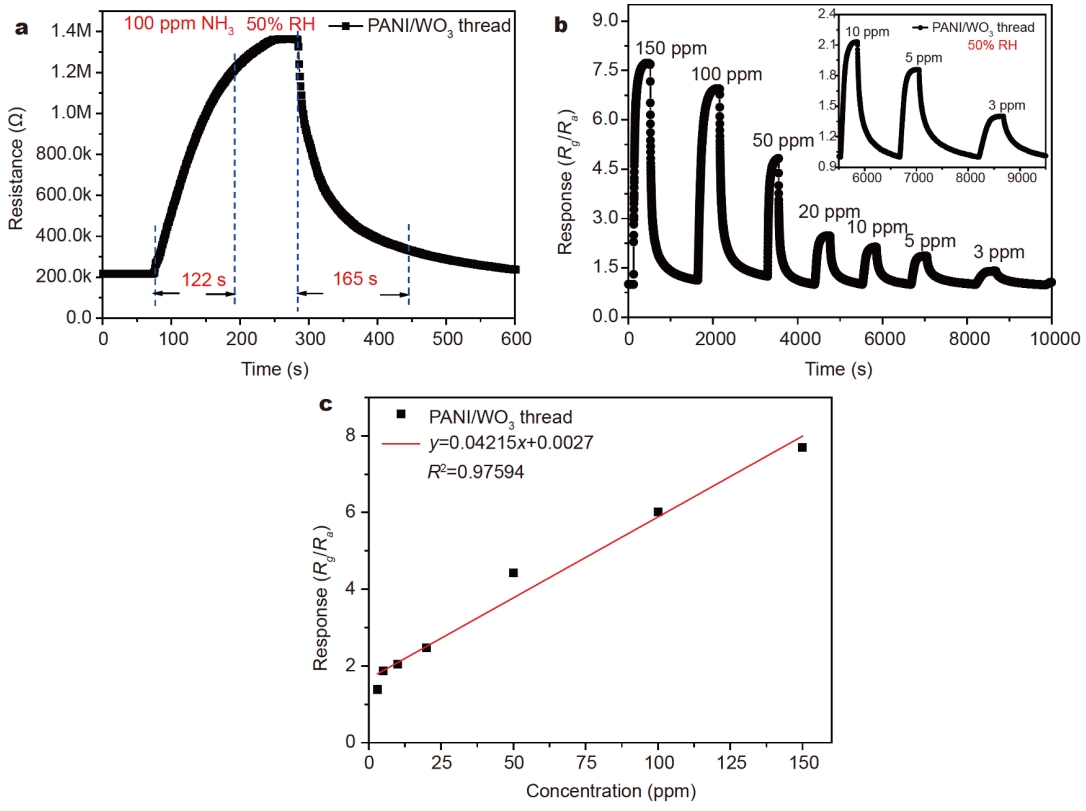

Figure 11 (a) The response-recovery curve of PANI/WO_3@cotton sensor to 100 ppm NH_3 at room temperature. (b) The dynamic response curve to different concentrations of NH_3, and (c) the calibration plot of response value *vs.* NH_3 concentration.

demonstrate that the response time for PANI/WO_3 cotton sensor is 122 s and the recovery time is 165 s, which verifies that this sensor can be employed as a fabric-based gas sensor in real applications. Fig. 11b plots the dynamic response of the PANI/WO_3@cotton sensor to different concentrations of NH_3 at room temperature. It is found that the PANI/WO_3@cotton sensor has good performance within the range of 3–150 ppm. When the PANI/WO_3@cotton sensor is exposed to 3 ppm NH_3, the gas response is still 1.25. The equation of linear regression (in Fig. 11c) is R_g/R_a = 0.04215C (NH_3) (ppm) + 0.0027 (R^2=0.97594). The limit of detection (LOD) was calculated based on the standard derivation (3σ) method:

$$\mathrm{LOD}=3\sigma/S, \quad (1)$$

where S is the slope of the calibration curve and σ is the standard deviation of the blank signals. The LOD of NH_3 for the PANI/WO_3@cotton sensor is 192 ppb.

To investigate the performance of the physical flexibility of the sensor, the PANI/WO_3 cotton thread in a straight and bent form was exposed to 100 ppm NH_3 and measured at room temperature. The results are presented in Fig. 12a and the PANI/WO_3@cotton sensors show similar sensitivities of 5.48 and 5.26 in the straight and bent states, respectively. Since PANI-based materials are susceptible to environmental humidity, the effects of humidity on the PANI/WO_3@cotton sensor to NH_3 were also investigated. As displayed in Fig. 12b, the gas response of the sensor intensifies as the environmental humidity increases and tends to stabilize when the relative humidity (RH) reaches 65%. The results demonstrate such a sensor can be potentially applied in flexible electronics.

Repeatability and stability are always important indicators of gas sensors. To investigate these aspects of the device, the PANI/WO_3@cotton sensor was exposed to 100 ppm NH_3 throughout 5 cycles test. The resulting curves, as presented in Fig. 12c, display the PANI/WO_3 cotton sensor cannot make a 100% recovery at room temperature, and the resistance of the cotton thread gradually increases in both air and the target gas ambient during the tests. The recorded resistances in ambient air are 0.20, 0.24, 0.27, 0.30 and 0.34 MΩ, respectively, while the corresponding resistances in the target gas are 1.20, 1.36, 1.48, 1.68 and 1.86 MΩ, respectively. In view of the gas response calculation formula, $S=R_g/R_a$, the sensitivities for each cycle are 6.0, 5.7, 5.5, 5.6 and 5.6, respec-

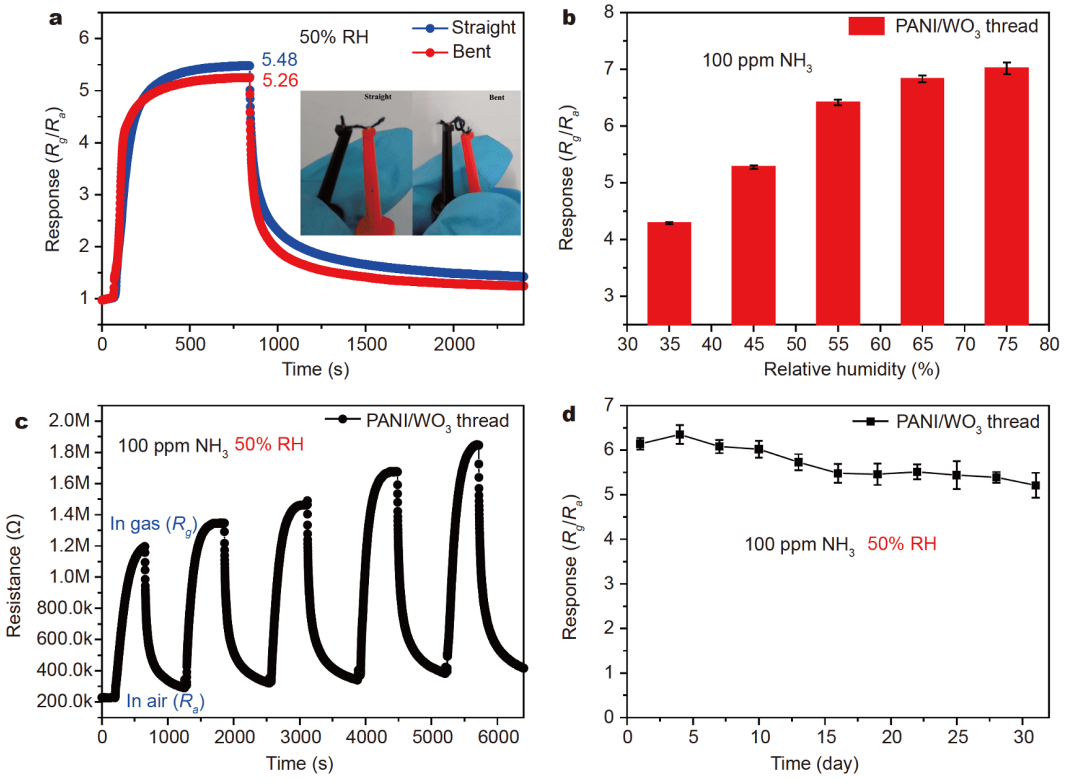

Figure 12 (a) The dynamic response curves for straight and bent PANI/WO_3 cotton thread, (b) the effect of humidity, (c) repeatability, and (d) stability of the PANI/WO_3@cotton sensor to 100 ppm NH_3 at room temperature.

tively. Hence the results illustrate the PANI/WO_3@cotton sensor exhibits efficient response/recovery performance with appropriate repeatability at room temperature. To further study the long-term stability of the PANI/WO_3@cotton sensor to 100 ppm NH_3, response/recovery cyclic tests were repeated over thirty days. The result in Fig. 12d demonstrates the gas response of the PANI/WO_3@cotton sensor slightly decreases from a value of 6.0 to 5.5. Therefore, the PANI/WO_3 cotton thread exhibits good long-term stability.

The sensing mechanism

The PANI/WO_3@cotton sensor has superior sensing performance for several reasons: (1) the deprotonation/protonation process of the pristine PANI, (2) the unique PANI/WO_3 composite structure, (3) the higher surface-to-volume ratio based on cotton thread, and (4) the increased protonation of PANI in the composites.

Firstly, it has already been noted that deprotonation/protonation plays an important role in the sensing performance of the pristine PANI [46], which mainly occurs in proton enriched environments, as illustrated in Fig. 13a. The PANI thread was treated by acid and then put into the NH_3 environment, with the protons in PANI extracted by NH_3 leading to the change of state. A conductive emeraldine salt state (ES form) of PANI is thus altered into an intrinsic emeraldine state (EB form), leading to the increment of resistance. Alternatively, once the acidified PANI thread is placed in an air atmosphere, the reaction process is then reversed, resulting in the decrease of resistance. In addition, the intrinsic polyaniline structure contains 1D organic main chain in the form of alternating single bond and double bond, and has no conductivity in the undoped state. p-Type semiconductor is formed after doping with SSA. Contacting with the reducing gas NH_3, the number of carriers (holes) in the material decreases due to the arc pair electrons in ammonia molecules, which are electron donors. NH^{4+} is formed on the surface of the material, which increases the potential barrier, hinders the movement of carriers and decreases the conductivity of the material, thus showing the sensitivity of the material to the target gas sensitivity [47,48].

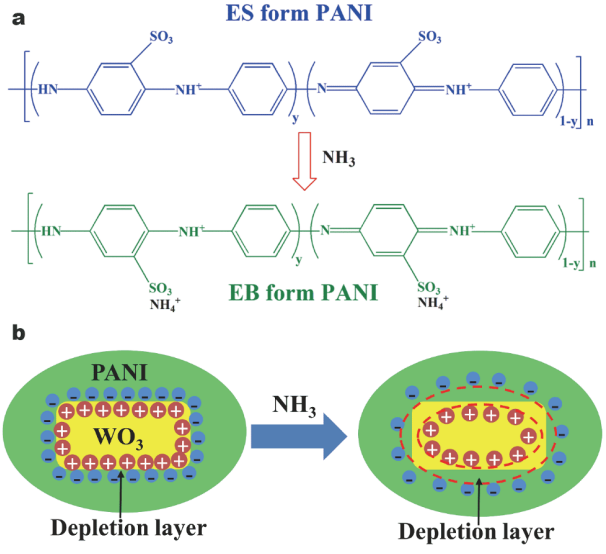

Figure 13 (a) Mechanism diagram of the interactions of NH_3 with pristine PANI and (b) changes of the depletion layer of the PANI/WO_3 nanocomposites before and after NH_3 adsorption.

Secondly, the gas response of the PANI/WO_3@cotton sensor to NH_3 shows a significant improvement, compared with that of the pristine PANI and WO_3, which may be attributed to the unique composite structure of PANI/WO_3. SEM images show that the surface of the acidified PANI thread is smooth with a limited number of nano-sheets. However, the surface of the PANI/WO_3 cotton thread is much coarser after being decorated with WO_3, thus providing more sufficient active sites for adsorption and diffusion, leading to a subsequent improvement in the sensing response. It is noted that WO_3 is a typical n-type semiconductor while acidified PANI is a p-type organic semiconductor. When the PANI nanoparticles are wrapped on the surface of WO_3, it leads to electron transfer from n-type WO_3 to p-type PANI, and the hole transfer from PANI to WO_3. This process results in a non-uniform carrier concentration on both sides of the WO_3 and PANI, and an internal electric field established between the interfaces of PANI and WO_3. A new Fermi level is formed in the PANI/WO_3 composite structure, as a stable p-n heterojunction and a narrow depletion layer are formed at the PANI and WO_3 interface [49]. The resistance of pure PANI (p-type) is 38 kΩ, while the resistance of pure WO_3 is 19 kΩ. However, after introducing different molar ratios of WO_3 to PANI, the resistances of PANI/WO_3 (5, 7.5, 10, 12.5 mol%) are 111, 198, 228, and 598 kΩ, respectively, which are much higher than that of pure PANI, evidencing the formation of the p-n junctions between PANI and WO_3 [50]. When the PANI/WO_3 cotton thread is exposed to NH_3, the gas extracts protons and destroys the PANI original state. During this process, the area of the depletion region at the heterogeneous interface of the PANI and WO_3 becomes thicker, resulting in a narrowing conduction path and a subsequent increase in resistance, as shown in Fig. 13b.

Thirdly, the adsorption and diffusion of NH_3 are directly related to the microstructure of the PANI/WO_3 cotton thread. The unique fiber structure exhibits a high surface-to-volume ratio and provides a greater number of adsorption sites for the NH_3 molecules [28]. Meanwhile, PANI is wrapped around the cotton forming a structure similar to a coaxial cable. The assembly can accelerate the one-way transmission of electrical signals, thus greatly improving the response and recovery ability.

Finally, according to EDX (Fig. 5), the PANI-WO_3 nanocomposite improves the protonation of PANI after introducing WO_3, due to the synergetic oxidation of WO_3 and APS. The increased protonation of PANI provides more $=NH^+$ groups for NH_3 molecule adsorption, and thus enhances the NH_3-sensing performance of the PANI/WO_3@cotton thread-based flexible sensor.

CONCLUSIONS

In this paper, we demonstrate the successful fabrication of a PANI/WO_3@cotton thread-based flexible sensor that is capable of detecting NH_3 at room temperature. The WO_3 nanoblocks were synthesized using a hydrothermal method, while the PANI/WO_3@cotton thread was prepared by *in-situ* polymerization. When the molar ratio of WO_3 is 10%, the sensor exhibits the highest gas response upon exposure to 100 ppm NH_3. The enhancement of gas response of the PANI/WO_3@cotton sensor can be explained as follows; firstly, the addition of WO_3 changes the microstructure of the PANI/WO_3@cotton thread as well as assists the protonation of the PANI material; secondly, the p-n heterojunctions are formed at the interface between the PANI and WO_3 regions; and finally, the high surface-to-volume ratio and parallel structure in the fabric substrate result in the increase of response. The PANI/WO_3@cotton sensor displays a high gas response of 6.0 to 100 ppm NH_3 at room temperature, as well as excellent selectivity, repeatability and stability properties. Furthermore, the bending of the fiber has negligible deterioration of the sensing performance. Therefore, the PANI/WO_3@cotton sensor demonstrates great potential as a flexible NH_3 sensor within the area of flexible and wearable electronics.

Received 10 February 2020; accepted 20 April 2020; published online 19 June 2020

1 Wang J, Li Z, Zhang S, *et al.* Enhanced NH_3 gas-sensing performance of silica modified CeO_2 nanostructure based sensors. Sens Actuat B-Chem, 2018, 255: 862–870
2 Nie Q, Pang Z, Li D, *et al.* Facile fabrication of flexible SiO_2/PANI nanofibers for ammonia gas sensing at room temperature. Colloids Surfs A-Physicochem Eng Aspects, 2018, 537: 532–539
3 Li S, Lin P, Zhao L, *et al.* The room temperature gas sensor based on polyaniline@flower-like WO_3 nanocomposites and flexible PET substrate for NH_3 detection. Sens Actuat B-Chem, 2018, 259: 505–513
4 Achary LSK, Kumar A, Barik B, *et al.* Reduced graphene oxide-$CuFe_2O_4$ nanocomposite: A highly sensitive room temperature NH_3 gas sensor. Sens Actuat B-Chem, 2018, 272: 100–109
5 Wu M, He M, Hu Q, *et al.* Ti_3C_2 MXene-based sensors with high selectivity for NH_3 detection at room temperature. ACS Sens, 2019, 4: 2763–2770
6 Wang X, Meng S, Tebyetekerwa M, *et al.* Nanostructured polyaniline/poly(styrene-butadiene-styrene) composite fiber for use as highly sensitive and flexible ammonia sensor. Synth Met, 2017, 233: 86–93
7 Sun Z, Liao T, Kou L. Strategies for designing metal oxide nanostructures. Sci China Mater, 2017, 60: 1–24
8 Hu X, Zhu Z, Chen C, *et al.* Highly sensitive H_2S gas sensors based on Pd-doped CuO nanoflowers with low operating temperature. Sens Actuat B-Chem, 2017, 253: 809–817
9 Kundu S, Kumar A. Low concentration ammonia sensing performance of Pd incorporated indium tin oxide. J Alloys Compd, 2019, 780: 245–255
10 He H, Zhang M, Zhao T, *et al.* A self-powered gas sensor based on PDMS/Ppy triboelectric-gas-sensing arrays for the real-time monitoring of automotive exhaust gas at room temperature. Sci China Mater, 2019, 62: 1433–1444
11 Mustapa R, Abu Mansor ZI, Sambasevam KP. Fabrication of polyaniline based chemical sensor for ammonia gas detection. JPS, 2018, 29: 9–16
12 Chopra S, Pham A, Gaillard J, *et al.* Carbon-nanotube-based resonant-circuit sensor for ammonia. Appl Phys Lett, 2002, 80: 4632–4634
13 Wang SG, Zhang Q, Yang DJ, *et al.* Multi-walled carbon nanotube-based gas sensors for NH_3 detection. Diamond Related Mater, 2004, 13: 1327–1332
14 Zhang Y, Xu P, Xu J, *et al.* NH_3 sensing mechanism investigation of CuBr: Different complex interactions of the Cu^+ ion with NH_3 and O_2 molecules. J Phys Chem C, 2011, 115: 2014–2019
15 Zhu Y, Cheng Z, Xiang Q, *et al.* Rational design and synthesis of aldehyde-functionalized mesoporous SBA-15 for high-performance ammonia sensor. Sens Actuat B-Chem, 2018, 256: 888–895
16 Li S, Xie L, He M, *et al.* Metal-organic frameworks-derived bamboo-like CuO/In_2O_3 heterostructure for high-performance H_2S gas sensor with low operating temperature. Sens Actuat B-Chem, 2020, 310: 127828
17 Das M, Sarkar D. One-pot synthesis of zinc oxide-polyaniline nanocomposite for fabrication of efficient room temperature ammonia gas sensor. Ceramics Int, 2017, 43: 11123–11131
18 Fratoddi I, Venditti I, Cametti C, *et al.* Chemiresistive polyaniline-based gas sensors: A mini review. Sens Actuat B-Chem, 2015, 220: 534–548
19 Wu J, Zhang Q, Zhou A, *et al.* Phase-separated polyaniline/graphene composite electrodes for high-rate electrochemical supercapacitors. Adv Mater, 2016, 28: 10211–10216
20 Yan H, Zhong M, Lv Z, *et al.* Stretchable electronic sensors of nanocomposite network films for ultrasensitive chemical vapor sensing. Small, 2017, 13: 1701697
21 Wan P, Wen X, Sun C, *et al.* Flexible transparent films based on nanocomposite networks of polyaniline and carbon nanotubes for

high-performance gas sensing. Small, 2015, 11: 5409–5415
22 Bai H, Shi G. Gas sensors based on conducting polymers. Sensors, 2007, 7: 267–307
23 Janata J, Josowicz M. Conducting polymers in electronic chemical sensors. Nat Mater, 2003, 2: 19–24
24 Tai H, Jiang Y, Xie G, *et al.* Influence of polymerization temperature on NH_3 response of PANI/TiO_2 thin film gas sensor. Sens Actuat B-Chem, 2008, 129: 319–326
25 Liu C, Tai H, Zhang P, *et al.* Enhanced ammonia-sensing properties of PANI-TiO_2-Au ternary self-assembly nanocomposite thin film at room temperature. Sens Actuat B-Chem, 2017, 246: 85–95
26 Bandgar DK, Navale ST, Navale YH, *et al.* Flexible camphor sulfonic acid-doped PANI/α-Fe_2O_3 nanocomposite films and their room temperature ammonia sensing activity. Mater Chem Phys, 2017, 189: 191–197
27 Wang L, Huang H, Xiao S, *et al.* Enhanced sensitivity and stability of room-temperature NH_3 sensors using core–shell CeO_2 nanoparticles@cross-linked PANI with p–n heterojunctions. ACS Appl Mater Interfaces, 2014, 6: 14131–14140
28 Li Y, Ban H, Jiao M, *et al. In situ* growth of SnO_2 nanosheets on a substrate *via* hydrothermal synthesis assisted by electrospinning and the gas sensing properties of SnO_2/polyaniline nanocomposites. RSC Adv, 2016, 6: 74944–74956
29 Wu S, Liu P, Zhang Y, *et al.* Flexible and conductive nanofiber-structured single yarn sensor for smart wearable devices. Sens Actuat B-Chem, 2017, 252: 697–705
30 Stoppa M, Chiolerio A. Wearable electronics and smart textiles: A critical review. Sensors, 2014, 14: 11957–11992
31 Labidi A, Jacolin C, Bendahan M, *et al.* Impedance spectroscopy on WO gas sensor. Sens Actuat B-Chem, 2015, 106: 713–718
32 Siciliano T, Tepore A, Micocci G, *et al.* WO_3 gas sensors prepared by thermal oxidization of tungsten. Sens Actuat B-Chem, 2008, 133: 321–326
33 Szilágyi IM, Wang L, Gouma PI, *et al.* Preparation of hexagonal WO_3 from hexagonal ammonium tungsten bronze for sensing NH_3. Mater Res Bull, 2009, 44: 505–508
34 Srivastava V, Jain K. Highly sensitive NH_3 sensor using Pt catalyzed silica coating over WO_3 thick films. Sens Actuat B-Chem, 2008, 133: 46–52
35 He M, Xie L, Zhao X, *et al.* Highly sensitive and selective H_2S gas sensors based on flower-like WO_3/CuO composites operating at low/room temperature. J Alloys Compd, 2019, 788: 36–43
36 Zhang J, Liu F, Gan J, *et al.* Metal-organic framework film for fluorescence turn-on H_2S gas sensing and anti-counterfeiting patterns. Sci China Mater, 2019, 62: 1445–1453
37 Zhang H, Wang Y, Zhu X, *et al.* Bilayer Au nanoparticle-decorated WO_3 porous thin films: On-chip fabrication and enhanced NO_2 gas sensing performances with high selectivity. Sens Actuat B-Chem, 2019, 280: 192–200
38 Li S, Diao Y, Yang Z, *et al.* Enhanced room temperature gas sensor based on Au-loaded mesoporous In_2O_3 nanospheres@polyaniline core-shell nanohybrid assembled on flexible PET substrate for NH_3 detection. Sens Actuat B-Chem, 2018, 276: 526–533
39 Xue L, Wang W, Guo Y, *et al.* Flexible polyaniline/carbon nanotube nanocomposite film-based electronic gas sensors. Sens Actuat B-Chem, 2017, 244: 47–53
40 Bai S, Zhao Y, Sun J, *et al.* Preparation of conducting films based on α-MoO_3/PANI hybrids and their sensing properties to triethylamine at room temperature. Sens Actuat B-Chem, 2017, 239: 131–138
41 Mane AT, Navale ST, Sen S, *et al.* Nitrogen dioxide (NO_2) sensing performance of *p*-polypyrrole/n-tungsten oxide hybrid nanocomposites at room temperature. Org Electron, 2015, 16: 195–204
42 Chen G, Chu X, Qiao H, *et al.* Thickness controllable single-crystal WO_3 nanosheets: Highly selective sensor for triethylamine detection at room temperature. Mater Lett, 2018, 226: 59–62
43 Bai S, Ma Y, Luo R, *et al.* Room temperature triethylamine sensing properties of polyaniline–WO_3 nanocomposites with p–n heterojunctions. RSC Adv, 2016, 6: 2687–2694
44 Kim MH, Jang JS, Koo WT, *et al.* Bimodally porous WO_3 microbelts functionalized with Pt catalysts for selective H_2S sensors. ACS Appl Mater Interfaces, 2018, 10: 20643–20651
45 Hu X, Zhu Z, Li Z, *et al.* Heterostructure of CuO microspheres modified with $CuFe_2O_4$ nanoparticles for highly sensitive H_2S gas sensor. Sens Actuat B-Chem, 2018, 264: 139–149
46 Kumar L, Rawal I, Kaur A, *et al.* Flexible room temperature ammonia sensor based on polyaniline. Sens Actuat B-Chem, 2017, 240: 408–416
47 Chabukswar VV, Pethkar S, Athawale AA. Acrylic acid doped polyaniline as an ammonia sensor. Sens Actuat B-Chem, 2001, 77: 657–663
48 Kukla AL, Shirshov YM, Piletsky SA. Ammonia sensors based on sensitive polyaniline films. Sens Actuat B-Chem, 1996, 37: 135–140
49 Pang Z, Nie Q, Zhu Y, *et al.* Enhanced ammonia sensing characteristics of CeO_2-decorated SiO_2/PANI free-standing nanofibrous membranes. J Mater Sci, 2019, 54: 2333–2342
50 Vasiliev RB, Rumyantseva MN, Yakovlev NV, *et al.* CuO/SnO_2 thin film heterostructures as chemical sensors to H_2S. Sens Actuat B-Chem, 1998, 50: 186–193

Acknowledgements This work was supported by the National Natural Science Foundation of China (61471233).

Author contributions He M and Xie L designed and engineered the samples and performed the experiments; Luo G and Li Z performed the data analysis; Wright J revised the paper; Zhu Z conceived this study. All authors contributed to the general discussion. All authors have given approval to the final version of the manuscript.

Conflict of interest The authors declare no conflict of interest.

Supplementary information Supporting data are available in the online version of the paper.

Meng He received her bachelor degree from Changchun Institute of Technology in 2016. Then she was continuing to pursue a master degree in Shanghai Polytechnic University and the University of Shanghai for Science and Technology. Her research focuses on the chemical gas sensors.

Lili Xie received her PhD degree in Shanghai Institute of Ceramics, Chinese Academy of Sciences (2005), where she worked on the synthesis, characterization and properties of molecular sieves. Since July 2005, she has been a lecturer in Shanghai Polytechnic University. She has published over 15 peer-reviewed journal papers so far and her main research interests are the gas sensing properties of inorganic nano-materials.

Zhigang Zhu received his PhD degree in Shanghai Institute of Ceramics, Chinese Academy of Sciences (2005), where he worked on functional materials and devices. In 2009–2012, he was a research associate at the University of Cambridge focusing on MEMS design and fabrication for biosensors. He became a Jinqiao Professor in Shanghai Polytechnic University in 2012, and joint Professor in the University of Shanghai for Science and Technology. He has published over 80 peer-reviewed papers so far and his main research interests are micro-/nano biosensors and chemical gas sensors.

基于p-型PANI/n-型WO_3异质结的柔性气体传感器及其室温下高性能NH_3检测

贺蒙[1,2†], 解丽丽[2†], 罗贵芳[2], 李崭虹[2], James Wright[3], 朱志刚[1,2*]

摘要 本文研制了一种能在室温下检测NH_3的PANI/WO_3@棉线传感器. 采用原位聚合的方法用PANI包裹WO_3, 并利用TEM、SEM、XRD和FTIR对样品的形貌和结构进行了研究. 研究了不同PANI与WO_3摩尔比的PANI/WO_3@棉线传感器在室温下对100 ppm氨气的传感性能, 结果表明, 最佳传感器(10 mol% WO_3)对100 ppm的NH_3灵敏度为6.0, 明显高于纯PANI及其他复合材料. 此外, PANI/WO_3@棉线传感器也显示出优异的选择性、灵敏性和柔韧性. 复合材料中独特的纤维结构、p-n异质结的形成以及PANI质子化程度的增加使得该传感器表现出优异的NH_3传感性能.

